Original Article

Bulletin of Pure and Applied Sciences.
Vol.37 C (Chemistry), No.2, 2018: P.187-194
Print version ISSN 0970 4620
Online version ISSN 2320 320X
DOI 10.5958/2320-320X.2018.00027.4

Studies of Isopropoxide Bridge Hetero-Bimetallic Complexes: Synthesis, Spectral, Morphology and Antimicrobial Activity

Manoj Kumar[1], Afreen Anjum[2], Sikandar Paswan[3], Raj Kumar Dubey[4],*

Author Affiliations:
[1-4]Synthetic Inorganic and Metallo-Organic Research Laboratory, Department of Chemistry, University of Allahabad, Allahabad 211002, India

***Corresponding Author:**
Raj Kumar Dubey, Synthetic Inorganic and Metallo-Organic Research Laboratory, Department of Chemistry, University of Allahabad, Allahabad 211002, India

E-mail: rajalkoxy@yahoo.com

Received on 22th January 2018
Accepted on 31th March 2018

Abstract

Equimolar reaction of $[M(sb)Cl]_2$ with sodium salt of $Al(OPr^i)_3$ affords the hetero-bimetallic complexes of the general formula $[M(sb)(\mu\text{-}OPr^i)_2Al(OPr^i)_2]$ **1-6** [where M = Cu, **1-3**; Co, **4-6**; sb = Schiff base; salicylidene-4-methyl-1-aminobenzene (smabH) **1**, **4**; salicylidene-1-aminobenzene (sabH) **2**, **5** and salicylidene-4-chloro-1-aminobenzene (scabH) **3**, **6**]. These complexes have been characterized by elemental analysis (C, H, N and Cu), IR, ESI-MS, ESR, PXRD and SEM-EDX studies. These hetero-bimetallic compounds were tested for their *in vitro* antimicrobial activity against *S. aureus* (MTCC 902), *P. aeruginosa* (MTCC 741) and *E. coli* (MTCC 1687) bacterial strains.

Keyword: Schiff base, Isopropoxide, Hetero-bimetallic, ESR, Antimicrobial.

1. INTRODUCTION

The application of Schiff base metal complexes covers a broad area of research in the field of catalytic as well as bioinorganic chemistry [1, 2]. The Schiff base complexes of cobalt and copper play a significant role in the field of bioinorganic chemistry such as antibacterial [3], antifungal [3], antioxidant [4] etc. In literature many hetero-bimetallic complexes were reported having different type of metal centers present in their backbone [5, 6]. Therefore their structures and reactivity are different from that of their monometallic precursors [7]. A large number of hetero-bimetallic alkoxide are reported which can be used as single-source precursors in the synthesis of oxide ceramics [8]. In recent years, the application of bridged alkoxide as secondary ligands attracted significant attention in main group and transition metal chemistry because of their role as building blocks in the ceramic materials obtained by sol–gel processing [9, 10].

The enriched reactivity of aluminium isopropoxide towards hydrolysis or nucleophilic attack in general, requires more precautions and adaptations when used as precursor for any synthesis [11, 12]. The approach of bridging binuclear Co/Cu and Al complexes with isopropoxide groups was doing well and adjusting the packed tetra coordinated transition state on each metal center by the bridging two isopropoxide groups. The greater reactivity towards nucleophilic attack is caused by the lower electronegativity and resulting higher Lewis acidity of the aluminium metals [9]. Taking note of all these facts, we put effort to develop the chemistry of isopropoxide bridged hetero-bimetallic complexes containing Schiff base. All these synthesized color solid complexes are highly moisture sensitive and soluble in polar organic solvent. The important antibacterial property of metal Schiff base complexes promoted to screen the antimicrobial activity of these hetero-bimetallic complexes.

In present course of investigation, we report herein the synthesis and spectroscopic characterization of isopropoxy bridge hetero-bimetallic complex. The representative synthetic route is given in scheme 1.

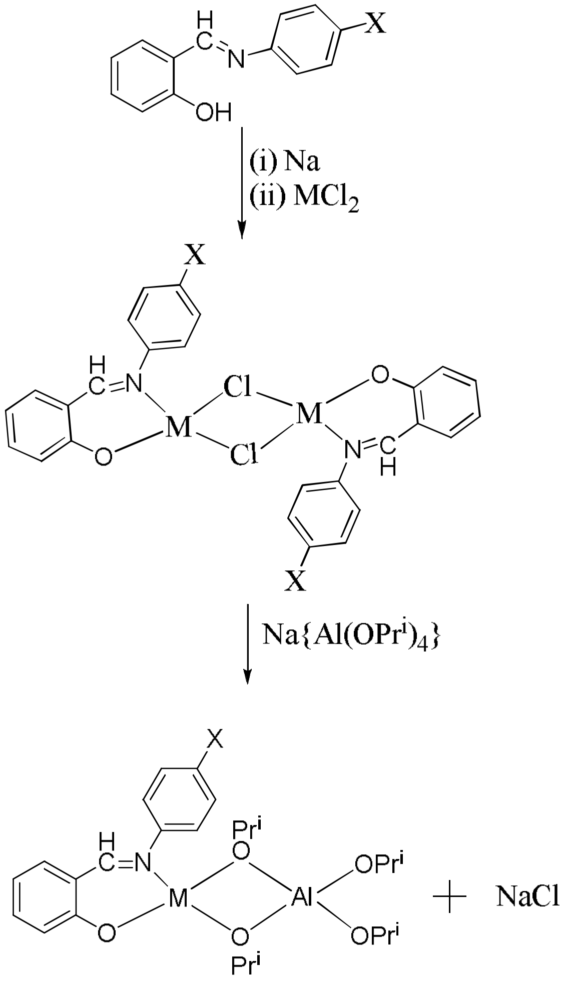

Scheme 1: Synthetic route for hetero-bimetallic complex, where X = CH_3 (**1**, **4**), H **(2**, **5)** and Cl **(3**, **6)**, M = Cu (**1-3)** and Co (**4-6).**

2. MATERIAL AND METHOD

2.1 Analytical methods and physical measurements

All chemicals used throughout the experiments were of AR and GR grade. All synthesis were carried out strictly under anhydrous condition. Solvents were purified and dried according to standard procedures describe in literature [12]. $[Na\{Al(OPr^i)_4\}]$ and $[M(sb)Cl]_2$ were synthesized as described in the literature [14, 15]. Cu was estimated gravimetrically as reported earlier through iodometric titration [16, 17]. The infrared spectra (4000–450 cm^{-1}) were recorded on a Perkin-Elmer 1000 FT-IR spectrophotometer. Elemental analyses were performed on Haraeous Carlo Erba 1108 elemental analyzer. Powder X-ray diffraction (PXRD) were recorded on X' Pert Pro XRD. HRMS were recorded in ESI mode. X band ESR spectra were done on JES-FA200 Spectrometer. SEM-EDX was recorded on JEOL, Japan (JFC 1600, Auto Fine Coater).

2.2 Synthesis of $[(sb)Cu(\mu\text{-}OPr^i)_2Al(OPr^i)_2]$ (1 - 3)

All synthesis were done according to standard literature procedure [14, 15]. A methanolic solution of $[Cu(smab)Cl]_2$ (1.00g, 1.61 mmol) was added to isopropanolic solution of $[Na\{Al(OPr^i)_4\}]$ (0.46g, 1.61 mmol) in 1:1 molar ratio(s). The stirring of resulting mixture was followed by refluxing over ~5h. The resulting solution was distilled and dried under reduced pressure. A colored crystalline product *[(smab)Cu(μ-OPr^i)$_2$Al(OPr^i)$_2$]* **1** was obtained. Similar procedures were adopted for synthesis of complexes **2** and **3**.

***[(smab)Cu(μ-OPr^i)$_2$Al(OPr^i)$_2$]* (1):** Yield, 48%; Anal. Found: C, 58.66; H, 7.73; N, 2.46; Cu, 11.43%. Calc. For $C_{27}H_{43}AlCuNO_5$; C, 58.73; H, 7.85; N, 2.54; Cu, 11.51%.
***[(sab)Cu(μ-OPr^i)$_2$Al(OPr^i)$_2$]* (2):** Yield, 53%; Anal. Found: C, 57.97; H, 7.52; N, 2.53; Cu, 11.71%. Calc. For $C_{26}H_{41}AlCuNO_5$: C, 58.03; H, 7.68; N, 2.60; Cu, 11.81%.
***[(scab)Cu(μ-OPr^i)$_2$Al(OPr^i)$_2$]* (3):** Yield, 44%; Anal. Found: C, 54.42; H, 6.98; N, 2.38; Cu, 11.01%. Calc. For $C_{26}H_{40}AlClCuNO_5$: C, 54.54; H, 7.04; N, 2.45; Cu, 11.10%.

2.3 Synthesis of *[(sb)Co(μ-OPr^i)$_2$Al(OPr^i)$_2$]* (4 - 6)

Similar procedures were done to synthesize complexes **4**, **5** and **6** as describe in 2.2.
***[(smab)Co(μ-OPr^i)$_2$Al(OPr^i)$_2$]* (4):** Yield, 47%; Anal. Found: C, 59.16; H, 7.83; N, 2.43%. Calc. For $C_{27}H_{43}AlCoNO_5$: C, 59.23; H, 7.92; N, 2.56%.
***[(sab)Co(μ-OPr^i)$_2$Al(OPr^i)$_2$]* (5):** Yield, 51%; Anal. Found: C, 58.45; H, 7.68; N, 2.52% Calc. For $C_{26}H_{41}AlCoNO_5$: C, 58.53; H, 7.75; N, 2.63%.
***[(scab)Co(μ-OPr^i)$_2$Al(OPr^i)$_2$]* (6):** Yield, 47%; Anal. Found: C, 54.88; H, 7.01; N, 2.36%. Calc. For C, $C_{26}H_{40}AlClCoNO_5$: 54.98; H, 7.10; N, 2.47%.

3. RESULT AND DISCUSSION

3.1 IR Spectra

The characteristic IR bands for all the complexes [M(sb)(μ-OPr^i)$_2$Al(OPr^i)$_2$] **1-6** when compared with those of its monometallic precursor, give positive indications about complex formation. A characteristic band observed in the region 800-900 cm^{-1} is due to bridging isopropoxide group between two metal centers [14]. A band in the region 1174 -1190 cm^{-1} is found due to terminal isopropoxide group. Some useful bands in all complexes are found in the region 1610-1630 cm^{-1}, 1440-1470 cm^{-1} and 1230-1260 cm^{-1} due to ν(C=N), ν(C=C) and ν(C-O) [15]. IR bands in the region 542-693 cm^{-1} are due to Al-O stretching [14].

3.2 ESI mass

The ESI mass spectra [18] of complexes [(smab)Cu(μ-OPr^i)$_2$Al(OPr^i)$_2$] **1** and [(smab)Co(μ-OPr^i)$_2$Al(OPr^i)$_2$] **4** {Figure 1(a) and (b)} were recorded in positive mode exhibiting peaks at m/z 553.4925 and 548.4213 due to complex [$C_{27}H_{43}AlCuNO_5$ + H]$^+$ (calcd. m/z 552.1616), and [$C_{27}H_{43}AlCoNO_5$ + H]$^+$ (calcd. m/z 547.5488) respectively. The result shows there is good 1:1 binding mode between Schiff base metal complex and aluminium isopropoxide.

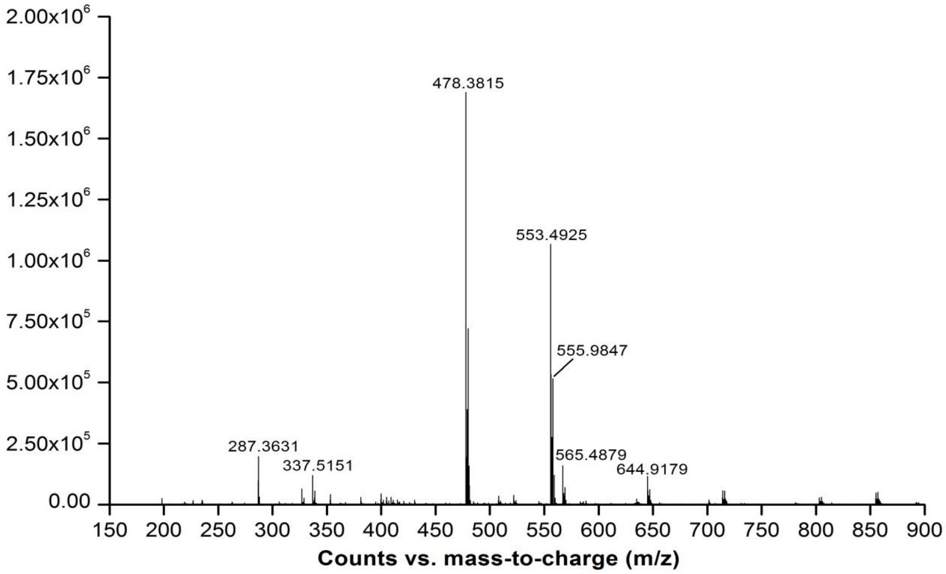

Figure 1 (a): ESI-MS spectra of complex [(smab)Cu(μ-OPr^i)$_2$Al(OPr^i)$_2$] (**1**).

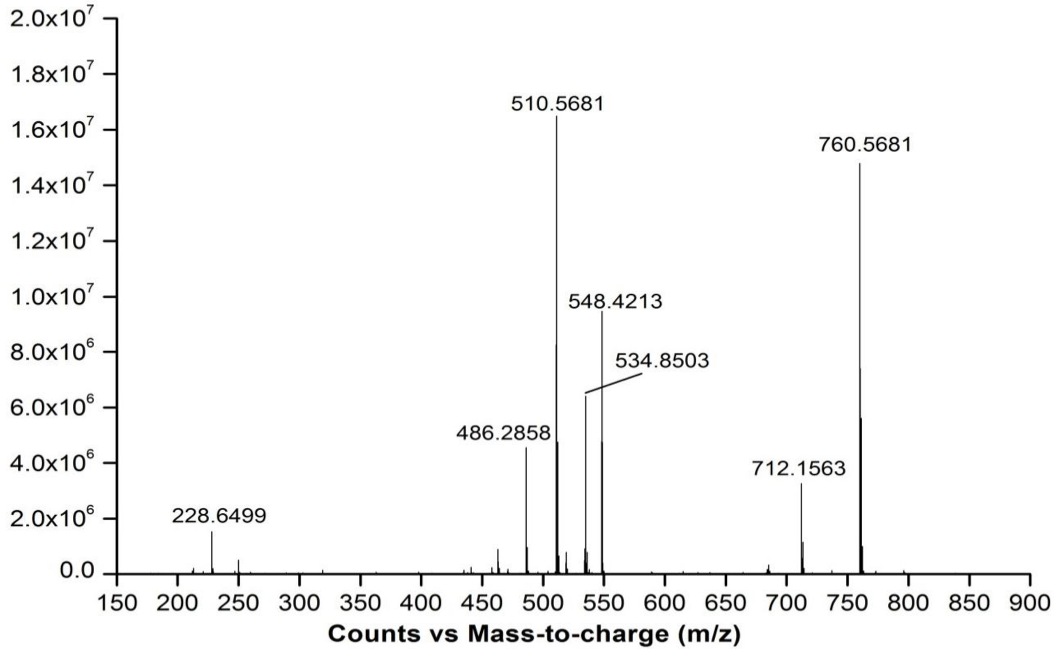

Figure 1 (b): ESI-MS spectra of complex $[(smab)Co(\mu\text{-}OPr^i)_2Al(OPr^i)_2]$ (**4**).

3.3 ESR spectra

To get information about the stereochemistry and the site of the metal ligand bonding, the X-band EPR spectrum (Figure. 2) of all copper (II) complex **1-3** were recorded at room temperature in methanolic solution. The different parameters are listed in table 2. The spin Hamiltonian parameters for the copper(II) complex is used to originate the ground state[19]. Kivelson and Neiman noted that the g_{II} value is an important function for indicating the metal–ligand bond character, for covalent character $g_{II} < 2.3$ and for ionic character $g_{II} > 2.3$, respectively [20]. All copper (II) complexes exhibited anisotropic signals with g_{II} values in the range 2.155–2.108 whereas the values of $g_\perp$ in the range 2.071–2.032. This shows the covalent metal–ligand bond character. The spectrum exhibited an isotropic signal with g_{av} = 2.0579(**1**), 2.0913(**2**) and 2.0875(**3**) calculated from the formula,

$$g_{av} = [g_{II} + 2g_\perp]/ 3$$

The trend of variation in the g values in the order $g_{II} > g_\perp > g_e$ (2.0023) showed that the unpaired electron is localized in the $dx^2{-}y^2$ orbital and predicts a square planar geometry around copper (II) ions [21].

The geometric value (G) is the measure of extent of exchange interactions and explained by Hathaway expression which stated that $G= (g_{II} - 2)/(g_\perp - 2)$. According to Hathaway and Billing, if the G value is greater than 4, the exchange interaction between the copper centers is negligible, whereas if its value is less than 4, the exchange interaction is noticed. A significant exchange coupling interaction between two copper (II) ions is present in solid complexes. This is usually the case for all copper(II) complexes with G value 3.35, 1.85 and 2.88 for complex **1**, **2** and **3**, respectively[21].

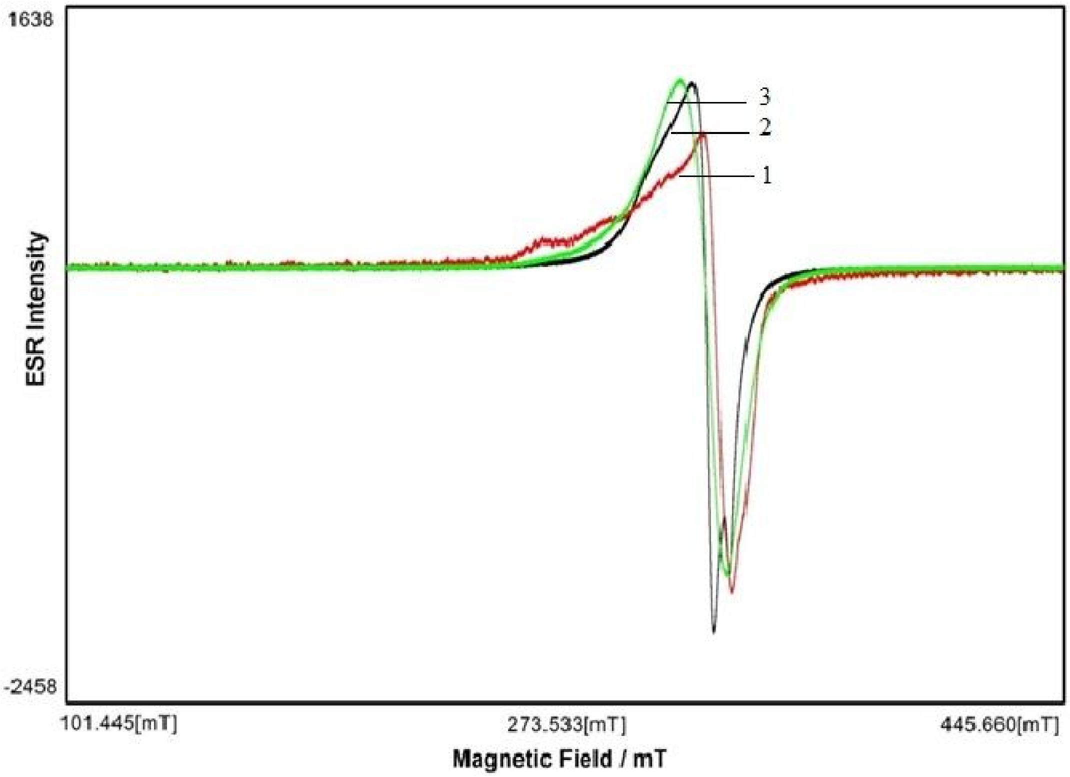

Figure 2: ESR spectra of complexes **1**-**3**.

Table 1: ESR data of copper complexes

S. N.	Complex	g_{II}	$g_{\perp}$	g_{av}	G
1	[(smab)Cu(μ-OPr^i)$_2$Al(OPr^i)$_2$] **1**	2.1089	2.0325	2.0579	3.3507
2	[(sab)Cu(μ-OPr^i)$_2$Al(OPr^i)$_2$] **2**	2.1319	2.0711	2.0913	1.8551
3	[(scab)Cu(μ-OPr^i)$_2$Al(OPr^i)$_2$] **3**	2.1554	2.0538	2.0875	2.8884

3.4 PXRD Spectra

The X-ray powder diffraction analysis [22] of the complexes has been performed in order to determine the structural information of polycrystalline material as it was difficult to isolate suitable single crystal for X-ray crystallography. The powder diffraction analysis of metal complexes **1**, **3** and **4** show amorphous in nature. The average crystallite size for the above mentioned complexes were calculated using Debye Scherrer's formula [22];

$D = 0.9\lambda/\beta.Cos\theta$

Where constant 0.9 is the shape factor, λ is the X-ray wavelength of Cu Ka radiation (1.5406 Å), θ is the Bragg diffraction angle and β is the full width at half maximum (FWHM). The experimental average grain sizes of **1**, **3** and **4** complexes were found to be 38.30, 24.25, 18.89 nm respectively.

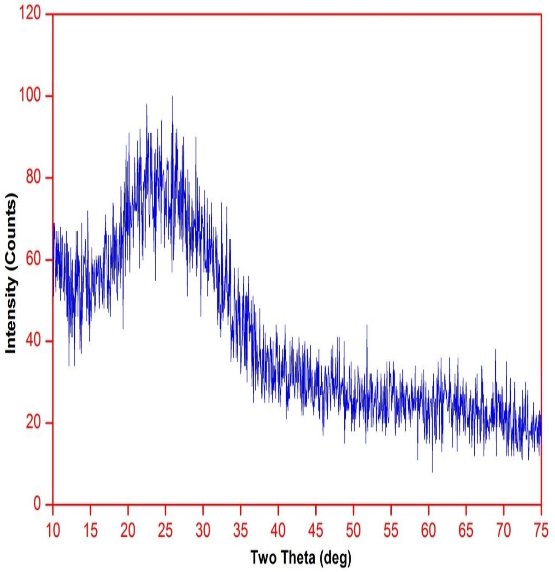

Figure 3(a): PXRD pattern of $[(smab)Cu(\mu\text{-}OPr^i)_2Al(OPr^i)_2]$ **1**.

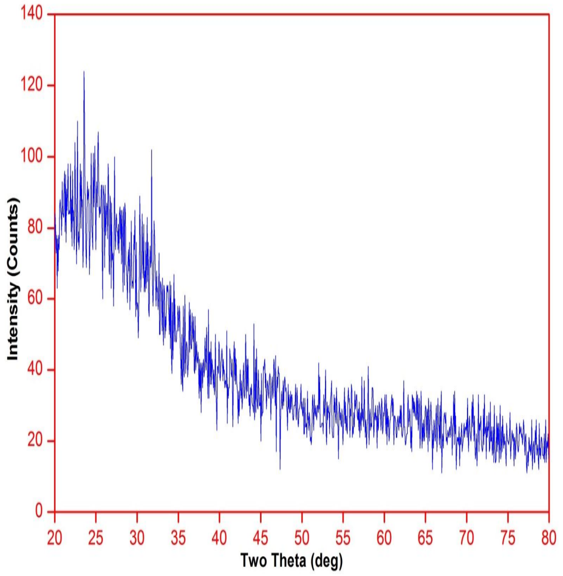

Figure 3(b): PXRD pattern of $[(smab)Co(\mu\text{-}OPr^i)_2Al(OPr^i)_2]$ **4**.

3.5 SEM-EDX analysis

The morphology of the hetero-bimetallic complexes has been illustrated by the scanning electron micrograph (SEM) [23]. The SEM micrographs of the complexes **1** is shown in figure 4(a). From the SEM micrographs it was noted that there is a uniform matrix showing rod like morphology. EDAX of complex **1**[Figure 4(b)] shows the presence of Cu and Al and other constituent indicated about purity of complexes.

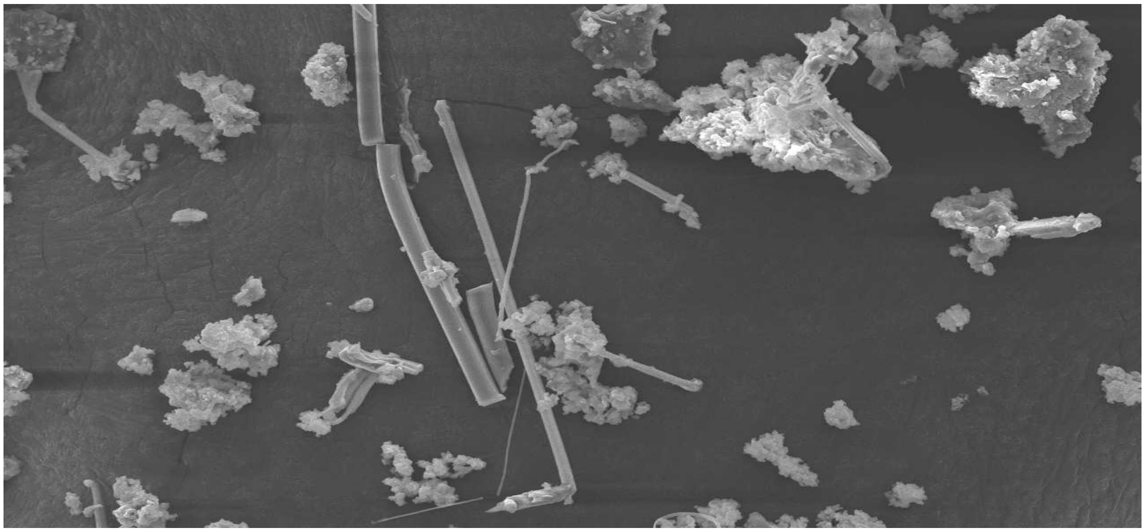

Figure 4(a): SEM and EDAX image of $[(sab)Cu(\mu\text{-}OPr^i)_2Al(OPr^i)_2]$ **3.**

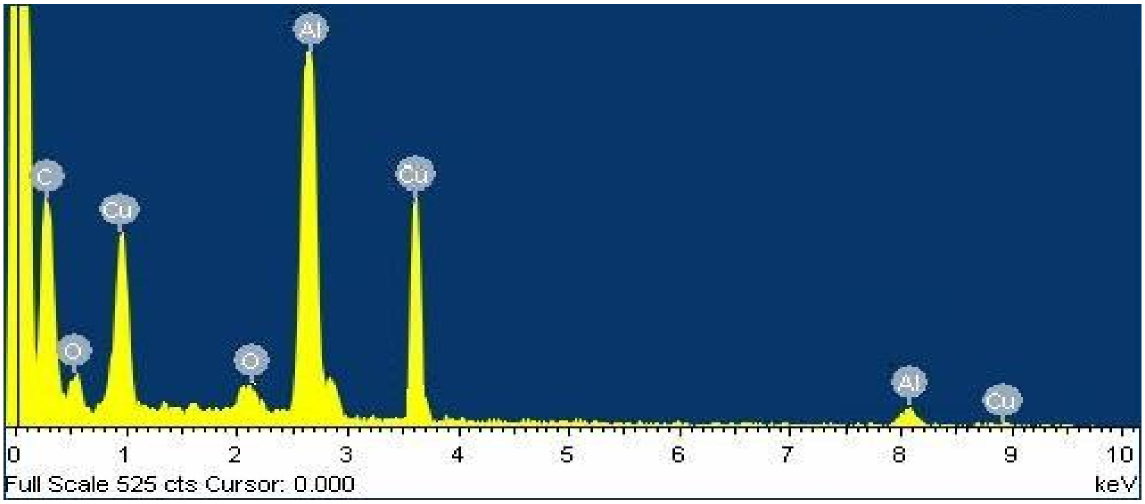

Figure 4(b): EDAX of $[(sab)Cu(\mu\text{-}OPr^i)_2Al(OPr^i)_2]$ **3.**

4. ANTIMICROBIAL ACTIVITY

The antibacterial activities [24] of complex **1** and **4** (named as AC3 and AC4) were screened against potential bacterial agents in methanolic solution with help of Agar well diffusion method. Pathogens against which antibacterial activity screened are *E. coli* (MTCC 1687), *P. aeruginosa* (MTCC 741) and *S. aureus* (MTCC 902). The antibacterial activities were established by the creation of clear inhibition zones around the discs which was measured in millimeters using a zone reader. The obtained results were compared with Tetracycline as standard reference drugs and given in table 2. The result shows moderate antibacterial activity of these complexes against all bacterial strain.

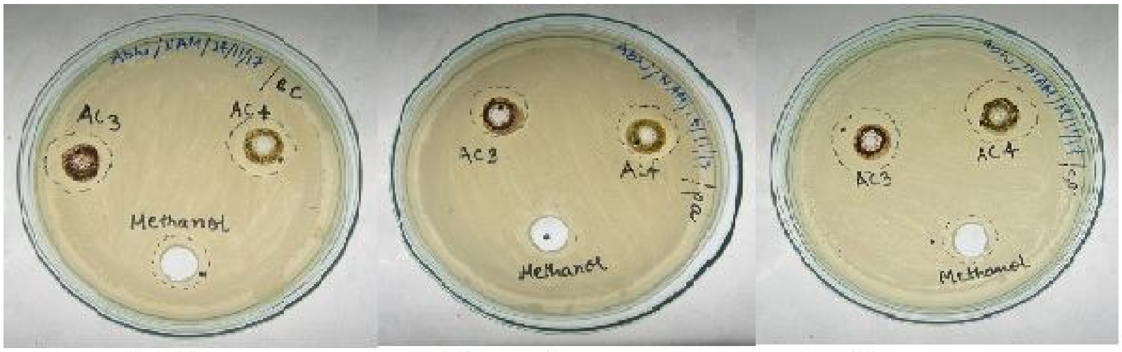

E.Coli *P. aeruginosa* *S. aureus*

Figure 5: Antibacterial activity of AC3(**1**), AC4(**4**) against three different pathogens (right to left; *E. coli, P. aeruginosa, S. aureus*) marked in a circle.

Table 2: Antibacterial activity of sample AC3 (**1**) and AC4 (**4**) against different pathogens

Zone Of Inhibition (mm)					
S. No.	**Pathogen**	**AC3 (1)**	**AC4 (4)**	**Methanol**	**Tetracyclin**
1.	*E. coli*	14mm	14mm	15mm	11.5mm
2.	*P. aeruginosa*	12mm	12mm	0	12mm
3.	*S. aureus*	15mm	16mm	10mm	11mm

5. CONCLUSION

In this paper, we report the synthesis, spectral, morphological and antimicrobial studies of isopropoxide bridge hetero-bimetallic complexes. Spectroscopic studies indicated about tetra coordination around each metal ion. ESR spectra of complexes **1-3** shows a square planar geometry around Cu(II) ion. PXRD shows amorphous nature of these complexes. SEM image shows a rod like morphology and EDAX indicated about purity of these complexes. These all complexes also show a moderate antibacterial activity.

6. ACKNOWLEDGEMENT

The authors (M.K., A.A. and S.P.) are thankful to UGC, New Delhi for providing financial assistant. The authors are also grateful to MNIT, Jaipur for recording IR, ESI-MS and PXRD, BBAU, Lucknow for SEM-EDAX, IIT, Bombay for recording ESR and MRD life sciences, Lucknow for screening antimicrobial activity.

7. REFERENCES

1. Lu, W-Y; Ou, H-W; Lee, C-N; Vandavasi, J. K.; Chen, H-Y; Lin, C-C. *Polymer*, 2018, *139*, 1-10.
2. Rudbari, H. K.; Iravani, M. R.; Moazam, V.; Askari, B.; Khorshidifard, M.; Habibi, N.; Bruno, G. *J. Mol. Struct*. 2016, *1125*, 113-120.
3. Sevgi, F.; Bagkesici, U.; Kursunlu, A. N.; Guler, E. *J. Mol. Struct*. 2018, 1154, 256-260.
4. Arif, R.; Nayab, P. S.; Ansari, I. A.; Shahid, M.; Irfan, M.; Alam, S.; Abid, M.; Rahisuddin *J. Mol. Struct.* 2018, *1160*, 142-153.
5. Hua, Y.; Guo, Z.; Han, H.; Wei, X. *Organometallics* 2017, *36*, 877−883.
6. Dubey, R. K.; Singh, A.; Mehrotra, R. C. *Inorg. Chim. Acta* 1986, *118*, 151-156.
7. Kurbah, S. D.; Kumar, A.; Syiemlieh, I.; Dey, A. K.; Lal, R. A. *J. Mol. Struct.* 2018, *1154*, 535-542.
8. Veith, M.; Mathur, S.; Lecerf, N.; Huch, V.; Decker, T. *J. Sol-Gel Sci. Technol.* 2000, *15*, 145–158.
9. Kickelbick, G. *Prog. Polym. Sci.* 2003, *28*, 83-114.
10. Pandey, S.; Mishra, S. B. *J. Sol-Gel Sci. Technol.* 2011, *59*, 73–94.
11. Lichtenberger, R.; Schubert, U. *J. Mater. Chem.* 2010, *20*, 9287–9296.
12. Dubois, Ph.; Jtrdme, R.; Teyssit, Ph. *Makromol. Chem., Macromol. Symp*. 1991, *42/43*, 103-116.
13. W. L. F. Argarego, D. D. Perrin, Purification of Laboratory Chemicals, 6th edition (Elsevier, 2009).
14. Dubey, R. K.; Baranwal, P. *Main Group Met. Chem.* 2011, *32(6)*, 321-340.
15. Dubey, R. K.; Mishra, C. M.; Mishra, A. N. *Indian J. Chem., Sect A* 2005, *44A*, 1159-1164.
16. Dubey. R. K.; Singh, A.; Mehrotra, R. C. *Transition Met. Chem.* 1985, *10*, 443-476.
17. A. I. Vogel, *A Text Book of Quantitative Inorganic Analysis*, 4th edn. (Longmans Green Co. Ltd. London, 1972).
18. Cheng, H-B; Huang, Y-D; Zhao, L.; Lia, X.; Wu, H-C. *Org. Biomol. Chem. 2015*, *13*, 3470-3475.
19. Chikate R. C.; Padhye, S. B. *Polyhedron* 2005, *24*, 1689–1700.
20. El-Boraey, H. A.; Abdel-Rahmanb, R. M.; Atia, E. M.; Hilmy, K. H. *Cent. Eur. J. Chem.* 2010, *8(4)*, 820–833.
21. Bharti, S.; Choudhary, M.; Mohan, B. *J. Coord. Chem.* 2018, *71(2)*, 284-310.
22. Sheikhshoaie, I.; Davaria, S.; Ramezanpour, S. *Chem. Method.* 2018, *3*, 46-54.
23. Modaberi, M. R.; Brahma, S.; Rooydell, R.; Wang, R-C; Liu, C-P. *Appl Organometal Chem.* 2017, *31*:e3746. DOI: 10.1002/aoc.3746.
24. Bagihalli, G. B.; Avaji, P. G.; Patil, S. A.; Badami, P. S. *Eur. J. Med. Chem.* 2008, *43*, 2639-2649.